American Mineralogist, Volume 83, pages 1256–1265, 1998

X-ray photoelectron spectroscopic study of a pristine millerite (NiS) surface and the effect of air and water oxidation

Daniel L. Legrand,[1,*] H. Wayne Nesbitt,[2] and G. Michael Bancroft[3]

[1]INCO Ltd., Central Process Technology, Copper Cliff, Ontario, POM 1N0, Canada
[2]Department of Earth Sciences, University of Western Ontario, London, Ontario, N6A 5B7, Canada
[3]Department of Chemistry, University of Western Ontario, London, Ontario, N6A 5B7, Canada

Abstract

Millerite, NiS, fractured under high vacuum and reacted with air and water has been analyzed by X-ray photoelectron spectroscopy (XPS). The pristine millerite surface gives rise to photoelectron peaks at binding energies of 853.1 eV (Ni $2p_{3/2}$) and 161.7 eV (S 2p), thus resolving ambiguities concerning binding energies quoted in the literature. Air-reacted samples show the presence of $NiSO_4$ and $Ni(OH)_2$ species. There is evidence for polysulfide species (S_n^{2-}, where $2 \leq n \leq 8$) on air-oxidized surfaces. These may occur in a sub-surface layer or may be intermixed with the $Ni(OH)_2$ in the oxidized layer. The $NiSO_4$ species at the millerite surface occur as discrete crystallites whereas the $Ni(OH)_2$ forms a thin veneer covering the entire millerite surface. The $NiSO_4$ crystallites form on the surface of millerite but not on surfaces of adjacent minerals. Surface diffusion of Ni^{2+} and SO_4^{2-} across the millerite surface is thought to be responsible for the transport and subsequent growth of $NiSO_4$ crystallites developed on millerite surfaces. Although it is clear that Ni and SO_4^{2-} does not diffuse onto surfaces of adjacent minerals in sufficient quantity to form crystallites, the explanation is uncertain. XPS results for water-reacted surfaces show little difference from the vacuum fractured surfaces with the exception that minor amounts of polysulfide and hydroxy nickel species are present. Similar reaction products to those formed in air [$NiSO_4$ and $Ni(OH)_2$] are believed to be produced, but these are removed from the millerite surface by dissolution, leaving behind a sulfur-enriched surface (polysulfide) and hydroxyl groups chemisorbed to nickel ions at the millerite surface.

Introduction

Millerite, NiS, is most commonly associated with other Ni-bearing sulfide minerals such as heazlewoodite (Ni_3S_2) and pentlandite $(Fe,Ni)_9S_8$. The oxidation of millerite is incompletely documented and there is some discrepancy in core-level binding energy values reported in the literature (Clifford et al. 1975; Shalvoy and Reucroft 1979; Broutin et al. 1984; Buckley and Woods 1991a). The present study attempts to reconcile ambiguities regarding core-level binding energies and to investigate millerite oxidation in air and in air-saturated de-ionized water.

The surface chemistry of millerite is significant because of its relationship with the surface chemistry of economically important Ni bearing sulfide minerals, and particularly because it can be considered a compositional Ni end-member of pentlandite and nickeliferous pyrrhotite, $Fe_{1-x}S$ ($0 < x < 0.2$). Its pristine and altered surface properties may consequently provide insight into the properties and reactivities of economically important Ni-bearing sulfides. This study documents the nature of a pristine millerite surface and its surface alteration properties resulting from reaction with the atmosphere and aerated deionized water. Processes affecting the formation of the secondary products are deduced and discussed. The results may provide a guide to the interpretation of surfaces and surface processes affecting other Ni-bearing sulfide minerals.

Experimental methods

Materials and instrumental methods

Millerite samples from Marbridge Mine in LaMotte township, Quebec, Canada, and Strathcona Mine near Sudbury, Ontario, Canada, were obtained from the Department of Earth Sciences mineral collection at the University of Western Ontario. The bulk composition was obtained by electron microprobe analysis (EMPA) of polished sections of millerite using a JEOL JXA-8600 Superprobe. The analyses were carried out with an accelerating voltage of 25 kV and a probe current of 25 nA as measured on a Faraday cup. ZAF matrix corrections were used. Counts were integrated for 20 s on peak and 20 s on background for nickel and sulfur, and for 30 s both on peak and on background for iron, copper, cobalt, and arsenic.

* E-mail: DLegrand@SUDBURY.Incoltd.com

0003–004X/98/1112–1256$05.00

X-ray photoelectron spectroscopic (XPS) analyses were performed using a Surface Science Laboratories SSX-100 X-ray photoelectron spectrometer with a monochromatized Al$K\alpha$ X-ray source (1487 eV). The instrument's work function was adjusted to give a value of 84.00 ± 0.05 eV for the Au $4f_{7/2}$ line of a gold foil standard. The spectrometer was calibrated such that the energy difference between the Cu $2p_{3/2}$ and Cu 3p lines of copper metal was 875.5 ± 0.1 eV. The position of the C 1s peak at 285.0 eV was monitored on each sample to ensure that no binding energy shift due to charging had occurred. The instrument base pressure in the analytical chamber was in the order of 10^{-6} to 10^{-7} Pa. Broad scans were collected using a spot size of 600 μm and a 150 eV analyzer pass energy. Narrow scans were collected at a 25 eV analyzer pass energy and a 300 μm spot size.

Scanning electron microscopy (SEM) analyses were conducted using a Hitachi model S-4500 Field Emission SEM. Energy Dispersive X-ray (EDX) analyses were performed on the same instrument with an EDAX™ Light Element Analyzer, which can detect elements with an atomic number greater than 4. The manufacturer's standardless quantification program was used.

Sample preparation

Pristine millerite samples were prepared by cleaving under ultra high vacuum (UHV), in the analytical chamber of the XPS instrument. The sample was cut into a parallelepiped and clamped into a vise-like sample holder. The end of the sample protruding from the holder was forced against the stainless steel lip of the analytical chamber's sample stage, thus cleaving the sample at about the level of the clamp. Broad scans and narrow scans were obtained immediately after cleavage.

Millerite samples used for the water oxidation experiments were cleaved in air and immediately immersed in de-ionized water. The de-ionized water experiment consisted of a covered Teflon vessel containing 50 mL of air saturated de-ionized water. The solution was stirred for the duration of the experiment. After 24 h, the samples were removed from the solution and rinsed with de-ionized water. The residual water was dabbed off with a Kim-wipe and the samples were immediately introduced to the XPS instrument for analysis.

The samples for the air oxidation experiment were cleaved in air and left on the laboratory benchtop for 24 h. Relative humidity and temperature in the laboratory were monitored, but not controlled, during the course of this experiment. The relative humidity ranged between 45 and 65% while the temperature was between 20 and 22 °C during the course of the experiments.

One millerite sample was polished with 0.25 μm diamond dust, rinsed with de-ionized water, wiped dry with a Kim-wipe, and left on the laboratory benchtop for 1 year. The relative humidity ranged between 30 and 80%, while the temperature was between 20 and 22 °C during the course of the experiment. As the purpose of the study is to determine the effects of reaction in natural setting and over a long period, there was no attempt to protect or otherwise modify the surfaces or to constrain the types of reactions that might have occurred.

Results

Electron microprobe results

EPMA gave a mean composition of 49.0 (3) at% Ni, 49.8 (3) at% S, 1.0 (1) at% Fe, and 0.1 (1) at% Co for millerite from Marbridge mine. The results for millerite from Strathcona mine were 49.0 (3) at% Ni, 50.0 (2) at% S, 0.4 (1) at% Fe, and 0.5 (1) at% Co. Cu and As were $<$0.1 at% for both samples.

X-ray photoelectron spectroscopy: Fitting constraints

Millerite is classified as a metallic conductor (Vaughan and Craig 1978) at room temperature, and its XPS spectra (Figs. 1–5) display characteristic asymmetric line shapes similar to those obtained for metals (Doniach and Sonjic 1970). The XPS spectra were therefore fitted using an asymmetric Gaussian-Lorentzian line shape. The asymmetric component to the line shape is required to fit all peaks and their high binding energy tail. The tail has been observed in other metallic sulfides such as heazlewoodite, Ni_2S_3 (Buckley and Woods 1991a), and covellite, CuS (Laajalehto et al. 1996). Also, because millerite exhibits Pauli paramagnetism (Vaughan and Craig 1978), there should be no unpaired electrons in the absence of a magnetic field, and one would not expect to see multiplet splitting in the XPS spectra of unaltered millerite.

All S 2p spectra show both the S $2p_{3/2}$ and S $2p_{½}$ components. Each doublet is constrained to have a binding energy difference of 1.18 eV between the S $2p_{3/2}$ and S $2p_{½}$ components, equal full width at half maximum (FWHM) values for both components, as well as a $2p_{3/2}$:$2p_{½}$ intensity ratio of 1.96:1 (Scofield 1976). All S 2p binding energy values are quoted for the S $2p_{3/2}$ component only.

A computer spreadsheet program, used to fit the XPS data, was written specifically to accept spectroscopic data, to allow fitting of Gaussian-Lorentzian line shapes, effects of spin-orbit splitting, Doniach-Sunjic high energy tails, Shirley backgrounds (Shirley 1972), and to evaluate the goodness of fit using χ^2 values. The peak parameters for the XPS results are shown in Table 1. Binding energies are reported to one decimal place and have an accuracy of ±0.2 eV. Table 2 contains XPS binding energy references for compounds of interest.

Identification of a secondary product

The SEM micrographs of the sample exposed to air for 1 year (Fig. 6) show small grains on the millerite grain but not the pentlandite surface. These small grains cannot be air-borne contaminants because they would have been deposited on both mineral surfaces. They must be secondary products of millerite that have crystallized at the millerite surface in response to reaction with atmospheric gases. An EDX analysis of a large crystallite revealed a composition of 16.2 at% Ni, 16.2 at% S, and 67.6 at%

TABLE 1. XPS S 2p, Ni $2p_{3/2}$, and O 1s peak parameters, proportions, and chemical state information for pristine and reacted millerite surfaces

Peak	B.E. (eV)	FWHM (eV)	Pristine (At%)	Reacted (at%) Water	Air (24 h)	Air (1 year)	Chemical state
S 2p*	161.7	0.75	100	93	57	0	monosulphide
S 2p*	162–164	1.6	0	7	9	0	polysulphide
S 2p*	168.8	1.6	0	0	34	100	sulphate
Ni $2p_{3/2}$	853.1	1.1	85	79	26	0	NiS
Ni $2p_{3/2}$	859.7	3.2	12	11	4	0	$NiS_{satellite}$
Ni $2p_{3/2}$	855.8	1.6	2	7	22	36	$Ni(OH)_2$
Ni $2p_{3/2}$	861.0	3.2	1	3	9	16	$Ni(OH)_{2\ satellite}$
Ni $2p_{3/2}$	856.7	1.6	0	0	27	33	$NiSO_4$
Ni $2p_{3/2}$	862.3	3.2	0	0	12	15	$NiSO_{4\ satellite}$
O 1s	531.5	1.4	0	0	43	43	hydroxyl
O 1s	531.9	1.5	57	64	0	0	$hydroxyl_{chemisorbed}$
O 1s	532.3	1.4	0	0	46	39	sulphate
O 1s	533–534	1.6–2.0	43	36	11	18	water

Note: Binding energies (B.E.) are reported relative to Au $4f_{7/2}$ at 84.00 eV.

* The S 2p binding energy is reported for the S $2p_{3/2}$ component. The S $2p_{1/2}$ component is at 1.18 eV higher binding energy with an intensity of 1/1.96 the intensity of the S $2p_{3/2}$ component. The S $2p_{1/2}$ peak is not listed in this table, but is used in fitting the XPS spectra in Figures 2, 3, 4, and 5.

O, which corresponds to a composition of $Ni_{1.0}S_{1.0}O_{4.2}$ when normalized to 1 mole of Ni. The result indicates an oxidized Ni-S salt with the proportions expected if Ni were divalent and sulfur was present as sulfate. The excess of oxygen may indicate that the $NiSO_4$ salt is somewhat hydrated, as would be expected considering the humidity of the laboratory. The identification is confirmed by the Ni 2p and S 2p XPS spectra of the 24 h and 1 year air-oxidized millerite samples. They demonstrate the presence of sulfate on these surfaces (discussed subsequently), thus corroborating the EDX results. The crystallites are a hydrated nickel-sulfate salt.

TABLE 2. XPS reference binding energies for Ni $2p_{3/2}$, S 2p, and O 1s lines

Species	Binding energy (eV) Ni $2p_{3/2}$	S 2p	O 1s	Reference
NiS	853.36	162.36		Clifford et al. 1975
	853.0	162.3		Shalvoy and Reucroft 1979
	854.2	162.1		Broutin et al. 1984
		161.6		Buckley and Woods 1991a*
$NiSO_4$	857.0	169.4		Shalvoy and Reucroft 1979
	858	169.4		Limouzin-Maire 1981
	856.5	168.5		Broutin et al. 1984
	858.0		532.0	Richardson and Vaughan 1989§
	857.3			Matienzo et al. 1973†
$NiSO_4 \cdot 6H_2O$	857.5			Matienzo et al. 1973†
Ni_3S_2	853.9	162.8		Broutin et al. 1984
	853.0	162.4		Buckley and Woods 1991a*
$Ni(OH)_2$			531.9	Broutin et al. 1984
	855.6		531.2	McIntyre and Cook 1975
	856.1		531.2	Salvati et al. 1981‡
	856.2		531.4	Löchel and Strehblow 1984‡
	856.2		531.0	Mansour 1996a‡
NiO	854.0		529.6	McIntyre and Cook 1975
	854.8		529.8	Salvati et al. 1981‡
	853.8		529.7	Löchel and Strehblow 1984‡
	854.0		529.6	Richardson and Vaughan 1989§
	854.5		529.6	Mansour 1996b‡
	855.0			Matienzo et al. 1973†
$Ni_2O_3 \cdot 6H_2O$	855.5		529.3	Mansour and Melendres 1996a‡
NiOOH	855.7		529.1^{oxide} $531.0^{hydroxide}$	Mansour and Melendres 1996b‡

* Original values relative to Au $4f_{7/2}$ = 83.8 eV.
† Original values relative to Au $4f_{7/2}$ = 83.0 eV.
‡ Original values relative to C 1s = 284.6 eV.
§ Unknown binding energy reference.

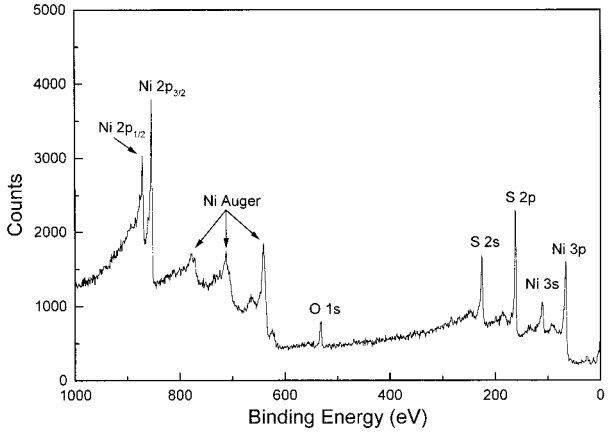

FIGURE 1. XPS broad scan of millerite cleaved under vacuum in the analytical chamber of the XPS instrument. The broad scan was collected immediately after cleavage. All major peaks are labeled. There is no detectable adventitious carbon contamination and oxygen is present in very small amounts. All other signals are derived from millerite.

INTERPRETATION OF XPS SPECTRA

Vacuum cleaved millerite

A small amount of oxygen (~10–15%) was present in the broad scan of a millerite surface cleaved in the vacuum chamber (Fig. 1). It is derived from the residual gases of the analytical chamber.

S 2p spectrum. The spectrum (Fig. 2a) is fitted with a doublet at 161.7 eV. This doublet is attributed to a nickel monosulfide species. S $2p_{3/2}$ binding energy values for NiS have been reported in the range 161.6 to 162.4 eV (Table 2). There is no evidence of polysulfide or oxidation of the sulfur species even though there is some oxygen on the surface. There appears to be a small contribution near 160.8 eV. This contribution is not always present, however, and may be due to the presence of a highly reactive surface state.

Ni $2p_{3/2}$ spectrum. The main Ni $2p_{3/2}$ peak (Fig. 2b) is located at 853.1 eV with a satellite peak near 859.7 eV. A small contribution (<5%) is required near 856 eV to obtain an adequate fit of this spectrum and this is an indication of a surface reaction product. Considering the composition of the mineral and the residual gases of the analytical chamber, only Ni oxides, hydroxides, or sulfates can be responsible for the Ni 2p photopeak in the region of 856 eV. Ni $2p_{3/2}$ binding energies for $Ni(OH)_2$ have been reported in the range of 855.6 to 856.2 eV (Table 2) and its presence, at low concentration, may explain the contribution near 856 eV. This is consistent with the observation of a small OH^- peak in the O 1s spectrum (Fig. 2c). Alternatively, the 856 eV peak may be due to shake-up (Briggs and Rivière 1994) but this does not explain the OH^- peak of the O 1s spectrum.

O 1s spectrum. The very weak O 1s spectrum of vacuum-fractured millerite (Fig. 2c) is fitted with two peaks, one at a binding energy of 531.9 eV and the second at 533.1 eV. Ni oxide peaks of Ni are located in the binding energy range of 529 to 530 eV (Table 2) whereas the binding energies of Ni-hydroxides are located at 531 to 532 eV (Table 2) and those of H_2O at still higher binding energies (Knipe et al. 1995). The absence of any appreciable intensity in the 529 eV–530 eV range of the O 1s spectrum provides good evidence for the absence of any oxide species at the millerite surface. The peak at 531.9 eV is attributed to a hydroxyl bonded to Ni^{2+} at the millerite surface and the peak at 533.1 eV is considered to arise from H_2O adsorbed to the millerite surface (Knipe

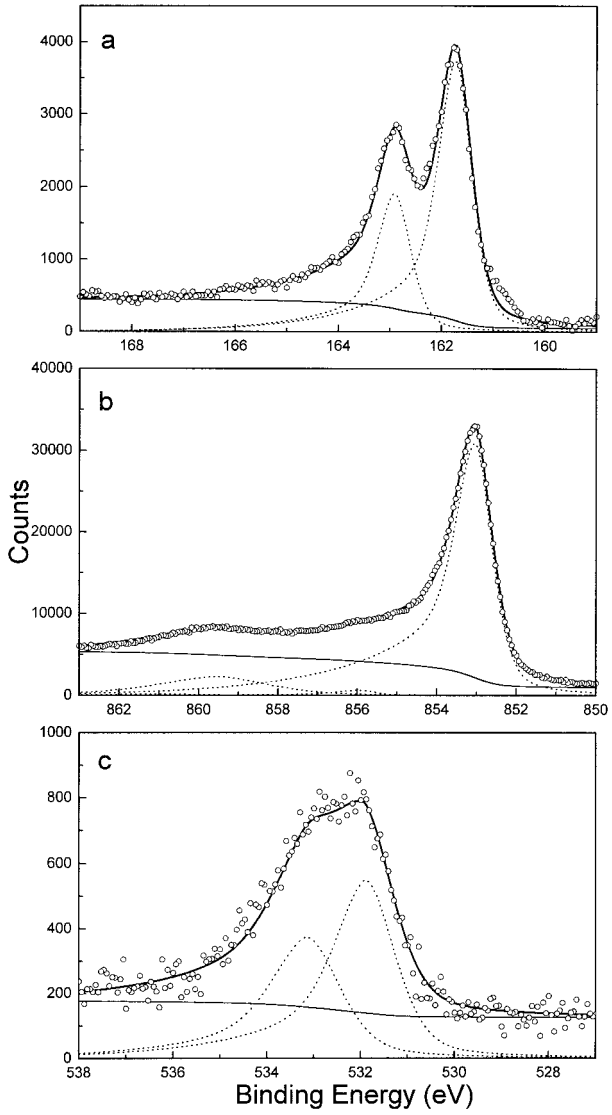

FIGURE 2. XPS S 2p (**a**), Ni $2p_{3/2}$ (**b**), and O 1s (**c**) narrow region scans of millerite cleaved under vacuum in the analytical chamber of the XPS instrument. The open circles represent raw data. The thick solid line is the fit to the experimental data. The thin solid line is the fitted Shirley background and the dashed lines represent photoemission peaks from the near-surface of millerite.

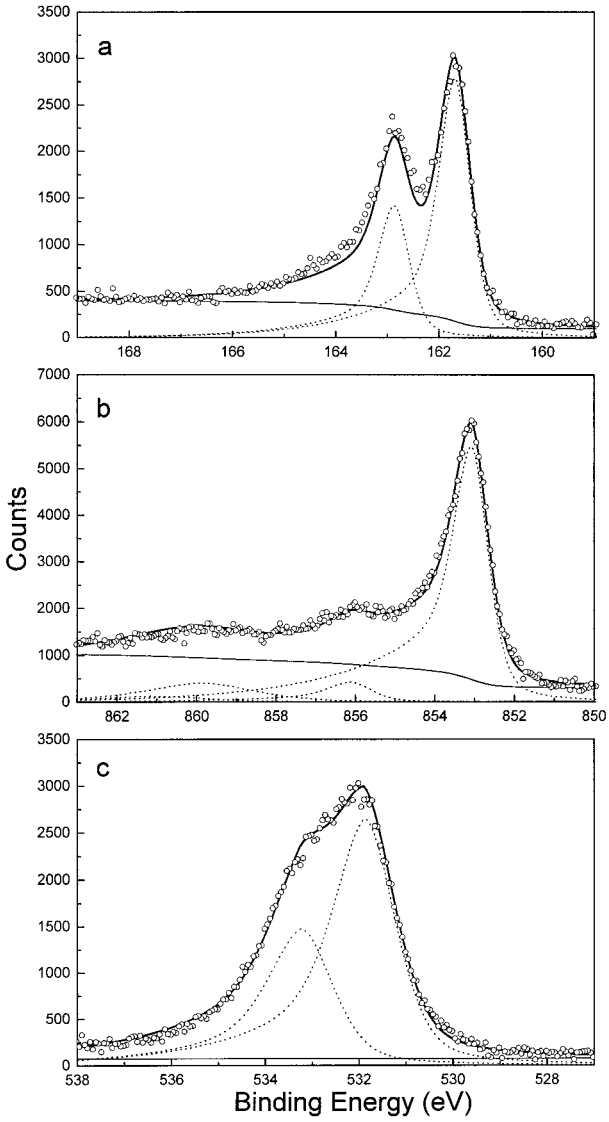

FIGURE 3. XPS S 2p (**a**), Ni $2p_{3/2}$ (**b**), and O 1s (**c**) narrow region scans of millerite reacted with de-ionized water for 24 h. See Figure 2 for symbols.

et al. 1995). These O 1s signals are considered to be the result from reaction of small amounts of residual water vapor in the vacuum chamber of the spectrometer with the freshly cleaved millerite surface. Although this evidence and XPS evidence from the water and air-reacted surfaces indicates the presence of hydroxide, the composition and nature of bonding associated with the Ni-hydroxide species is uncertain.

Water-reacted millerite—24 hours

S 2p spectrum. The S 2p spectrum of the water-reacted surface (Fig. 3a) was fitted using only the millerite monosulfide doublet at 161.7 eV. The intensity of this peak was adjusted to fit the spectral data for S $2p_{3/2}$ peak at 161.7 eV (Fig. 3a). Although the fit is good for this portion of the spectrum, the region around the S $2p_{½}$ peak, and particularly the high-energy side of this peak, is poorly fitted (compare XPS data and solid curve of Fig. 3a). An additional contribution (~7% of the total intensity, Table 1) is required to obtain an adequate fit between 162 eV and 165 eV. This is the region in which polysulfides (S_n^{2-}, where $2 \leq n \leq 8$) and elemental sulfur occur (Termes et al. 1987; Buckley et al. 1988; Mycroft et al. 1990; Bancroft and Hyland 1990; Pratt et al. 1994a). Oxysulfur species are generally observed at binding energies >165 eV and are therefore not a likely explanation. The additional contribution is consequently assigned to polysulfides and elemental sulfur but this requires confirmation.

Ni $2p_{3/2}$ spectrum. The Ni $2p_{3/2}$ spectrum of millerite that reacted for 24 h with aerated, de-ionized water (Fig. 3b) is similar to that of the pristine surface (Fig. 2b) except that the contribution centered about 856 eV is somewhat stronger. The major peak (853.1 eV) and its associated satellite (860 eV) is that of Ni^{2+} bonded to sulfur. The small contribution at 856 eV has been already interpreted as Ni^{2+} bonded to hydroxide (Fig. 2b). It has increased from 2% on the vacuum-fractured surface to about 7% on the water-reacted surface (Table 1). This is also consistent with the enhanced hydroxyl contribution to the O 1s spectrum (Fig. 3c). Although the Ni signal from $NiSO_4$ should also occur in this region there is no evidence for sulfate in the S 2p spectrum (Fig. 3a).

To verify the XPS results, Auger survey scans were collected before and after the reacted millerite surface was sputtered by an Ar^+ ion beam. The surface composition obtained before sputtering was 16 at% Ni, 14 at% S, 9 at% O, and 61 at% C, and after sputtering was 28 at% Ni, 43 at% S, 2 at% O, and 27 at% C. The decreased oxygen signal after sputtering confirms that the reacted surface is oxygen rich. The Auger results are therefore consistent with the XPS data.

O 1s spectrum. As for the vacuum-fractured surface, there is no discernible peak in the region of 529–530 eV so that oxide apparently is absent from this surface. The O 1s XPS narrow region scan of water-reacted millerite (Fig. 3c) was, however, fitted with 2 peaks at 531.9 eV and 533.2 eV (Table 1). These same peaks were observed in Figure 2c. The peak at 531.9 eV is consequently attributed to a hydroxyl group chemisorbed to nickel at the millerite surface, and the peak at 533.2 eV considered to arise from H_2O adsorbed onto the surface. The intensity of the hydroxyl peak is greater than that of the surface H_2O peak, which suggests that a greater proportion of surface oxygen is attributable to surface hydroxy nickel complexes.

Air-oxidized millerite—24 hours

S 2p spectrum. Comparison with Figure 3a demonstrates that the main peak of the S 2p spectrum of the surface reacted with air for 24 h (Fig. 4a) is due primarily to the millerite monosulfide contribution at 161.7 eV. There is, however, a significant contribution (9%) required to obtain a good fit in the range of 162–165 eV.

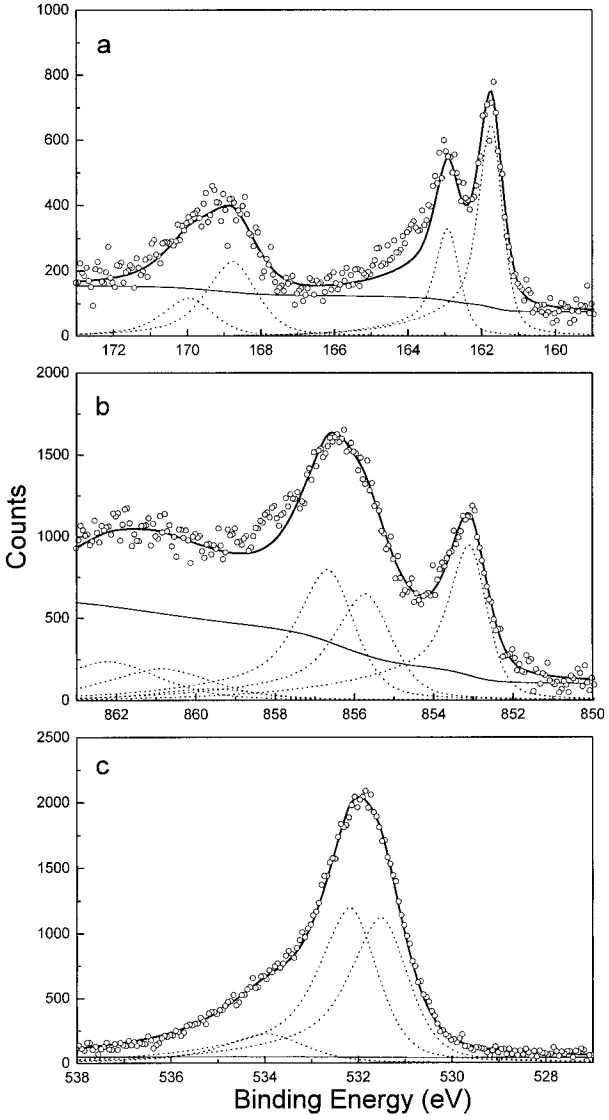

FIGURE 4. XPS S 2p (**a**), Ni $2p_{3/2}$ (**b**), and O 1s (**c**) narrow region scans of millerite exposed to air on a lab bench for 24 h. See Figure 2 for symbols.

As for the water reacted surface (Fig. 3a), this contribution is probably due to polysulfides (S_n^{2-}, where $2 \leq n \leq 8$) and elemental sulfur. There is also a significant contribution (34%) at 168.8 eV. This is the region in which the sulfate photopeak is observed (Table 2). The S 2p binding energies for $NiSO_4$ have been reported in the range of 168.5 to 169.4 eV (Table 2) and $NiSO_4$ crystallites have been identified on the millerite surface reacted with air for 1 year. The photopeak at 168.8 eV undoubtedly arises from a surface sulfate species, most likely $NiSO_4$. H^+ may also act as cation (an acidic surface component may also be present). The Ni 2p region provides additional support for the presence of $NiSO_4$ in the near-surface.

Ni $2p_{3/2}$ spectrum. The major peak of the Ni $2p_{3/2}$ spectrum for millerite exposed to air for 24 h (Fig. 4b) is at 853.1 eV and, by analogy with Figure 2b, it is attributed to Ni^{2+} bonded to monosulfide of millerite. The large signal at 856 eV is very broad, indicating that it is a composite peak. Ni $2p_{3/2}$ binding energy values for $Ni(OH)_2$ have been reported between 855.6 and 856.2 eV and Ni $2p_{3/2}$ binding energy values for $NiSO_4$ have been reported in the range of 856.5 to 858.0 eV (Table 2). There is clear evidence for SO_4^{2-} from the S 2p spectrum and as discussed subsequently, there is good evidence for OH^- from the O 1s spectrum (Fig. 4c). The broad peak at 856 eV consequently has been fitted with two peaks, one at 855.8 eV assigned to a $Ni(OH)_2$ surface species as observed on the cleaved and water-reacted surfaces (Fig. 2b and Fig. 3b), and a second peak at 856.7 eV assigned as $NiSO_4$ as identified on the 1 year, air-oxidized sample.

The signal near 856 eV may also arise from Ni^{3+} species. Binding energies for Ni^{3+} oxides and oxyhydroxides have been reported in the range of 855.5 to 855.7 eV (Table 2). The most common, and only naturally occurring oxidation state of nickel is Ni^{2+}. Very few compounds containing higher oxidation states exist (Cotton and Wilkinson 1988) because oxidation of nickel to higher oxidation states (>2) usually requires strong oxidants or electrochemical treatment. In our experiment, no strong oxidant came in contact with the sample, nor was the sample electrochemically oxidized, making the possibility of Ni^{3+} unlikely. Although the fit obtained with these two surface alteration species is reasonable there is an additional, small contribution near 858 eV that cannot be explained by the two surface species. Its explanation is uncertain.

O 1s spectrum. The O 1s XPS narrow scan for millerite exposed to air for 24 h (Fig. 4c) has been fitted using three peaks. One peak (531.5 eV) is attributed to a surface Ni-hydroxide species [$Ni(OH)_2$]. The binding energy value is consistent with those reported for $Ni(OH)_2$, which range from 531.0 to 531.4 eV (Table 2). A second peak, at 532.3 eV, is attributed to sulfate (as $NiSO_4$), and the binding energy is consistent with reported literature values (Table 2). They contribute 43 and 46%, respectively, of the total O 1s intensity of Figure 4c. These same two contributions [$Ni(OH)_2$ and $NiSO_4$] are observed on the 1 year air-reacted surface (Fig. 5c). The third contribution is represented by a peak at 534 eV (Fig. 4c) and constitutes 11% of the total O 1s intensity. It is assigned as water adsorbed onto the millerite surface (Knipe et al. 1995).

Air oxidized millerite—1 year

The sample was largely unprotected from natural airborne gases of the laboratory and indeed all atmospheric gases must have alighted on the surface. In spite of its long reaction time with a complex natural gas mixture, the sample yields interpretable XPS spectra (Fig. 5). Furthermore, the SEM/EDX observations discussed in the results section are a great aid to interpretation of these spectra because of the unambiguous identification of

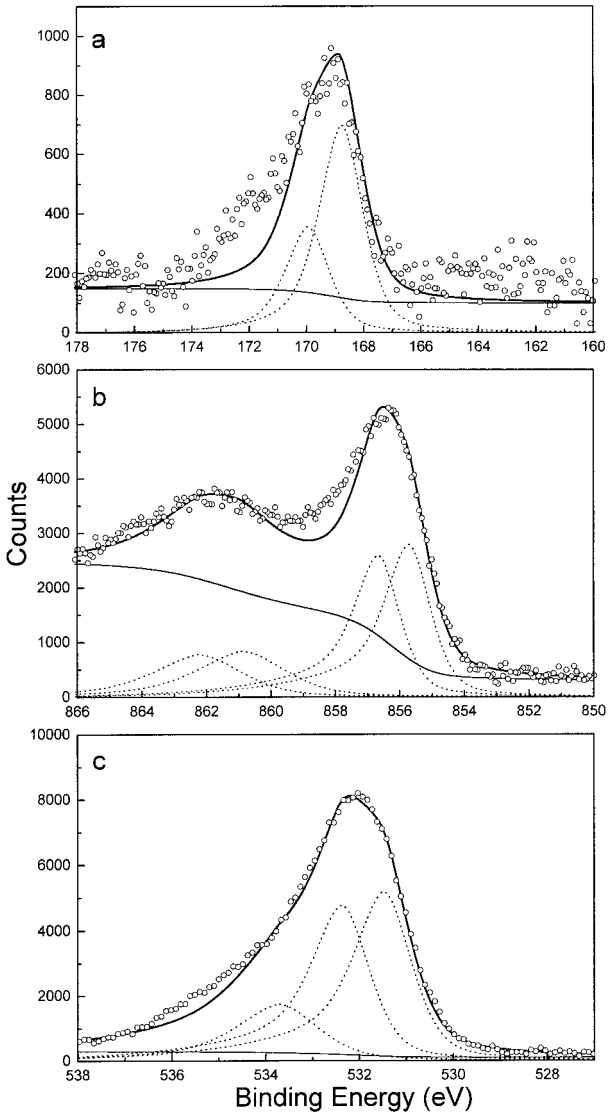

FIGURE 5. XPS S 2p (**a**), Ni $2p_{3/2}$ (**b**), and O 1s (**c**) narrow region scans of millerite exposed to air on a lab bench for 1 year. See Figure 2 for symbols.

nickel sulfate crystallites developed on the millerite surface (but not developed on the surfaces of adjacent mineral grains).

S 2p spectrum. The S 2p XPS spectrum (Fig. 5a) has a main peak at 168.8 eV, as observed on the 24 h air-oxidized surface (Fig. 4a). It is undoubtedly due to a sulfate photopeak as a $NiSO_4$ salt has been identified by SEM/EDX on this surface. The binding energy is consistent with reported literature values (Table 2). Although there may be a small contribution around 162–163 eV, it is masked by a noisy baseline and no peak has been included in this region of the fit. The intensity near 171 to 173 eV in the S 2p spectrum (Fig. 5a) is believed to arise from $NiSO_4$ crystallites in poor electrical contact with the surface. The result of this poor electrical contact is the accumulation of positive charge at the $NiSO_4$ crystallite surface, leading to peak shifts toward higher binding energy. A similar binding energy shift is observed in the Ni $2p_{3/2}$ spectrum (Fig. 5b) for this sample.

Ni $2p_{3/2}$ spectrum. The Ni $2p_{3/2}$ XPS narrow region scan of millerite exposed to air for 1 year is shown in Figure 5b. As for the 24 h air-oxidized sample, there is a strong, broad signal at around 856 eV indicating a composite peak. This signal is fitted with near equal contributions of $Ni(OH)_2$ at 855.8 eV and $NiSO_4$ at 856.7 eV. The intensity around 861–862 eV is due to satellite peaks. The contribution near 857.5 to 859.5 eV is believed to arise from $NiSO_4$ in poor electrical contact with the surface, giving rise to peaks shifted to higher binding energy. This is consistent with the results obtained for the S 2p spectrum (Fig. 5a). There is no indication of a Ni^{2+} signal from unaltered millerite, indicating that the oxidized overlayer is thicker than the attenuation length of Ni photoelectrons.

O 1s spectrum. This spectrum (Fig. 5c) is fitted using three peaks. There is no evidence for oxide (529–530 eV). The first peak, at 531.5 eV, is attributed to the presence of hydroxide [as $Ni(OH)_2$] at the surface. Binding energy values for $Ni(OH)_2$ are found in the range of 531.0 to 531.4 eV (Table 2). The second peak, at 532.3 eV, is attributed to sulfate (as $NiSO_4$). These contributions represent approximately 43 and 39% of the total O 1s intensity, respectively. The presence of $Ni(OH)_2$ and $NiSO_4$ is consistent with the observed contributions from the Ni $2p_{3/2}$ (Fig. 5b) and S 2p (Fig. 5a) spectra. The last contribution, representing approximately 18% of the total O 1s intensity, is fitted with a peak near 534 eV. This contribution is assigned as water adsorbed onto the millerite surface.

DISCUSSION

The air-oxidized millerite samples show convincing evidence for the formation of at least two distinct oxidation products, $NiSO_4$ and $Ni(OH)_2$. The S 2p XPS spectra (Fig. 4a and Fig. 5a) indicate the presence of sulfate and SEM/EDX analysis of the sample reacted with air for 1 year demonstrates that discrete crystallites of $NiSO_4$ have formed at the surface (Fig. 6). These crystallites are difficult to explain unless there is appreciable diffusion of Ni^{2+} and SO_4^{2-} across the oxidized surface. These constituents must have diffused to sites of nucleation and subsequent diffusion resulted in their growth to micrometer size (Fig. 6b).

The presence of $NiSO_4$ can be explained through oxidation of the sulfide ion in millerite to sulfate by molecular oxygen according to the following scheme:

$$NiS + 2O_2 \rightarrow NiSO_4.$$

In fact, it is most likely that the salt is hydrated. The presence of water in the O 1s spectrum supports the suggestion. The free energy of formation of hydrated $NiSO_4$ species is about 300 to 400 kcal/mol more negative than

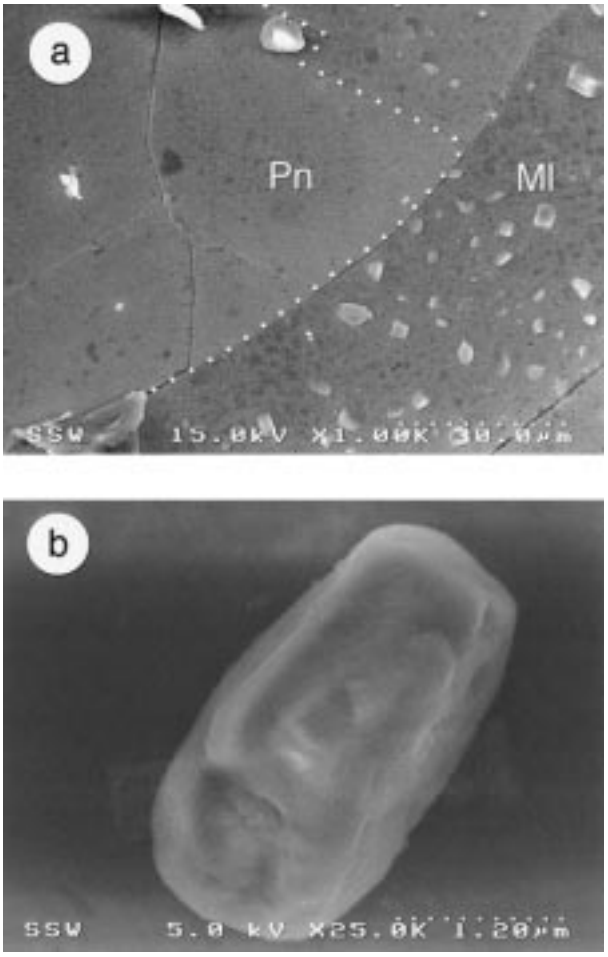

FIGURE 6. Field emission secondary electron micrographs of millerite exposed to air for 1 year. (**a**) Low magnification image of the millerite (Ml) and pentlandite (Pn) surfaces. The boundary separating the two phases is accentuated by the white dots. The millerite surface (Ml) is mottled (light and dark gray), with $NiSO_4$ crystallites distributed over the surface. The pentlandite surface (Pn) is less mottled and is virtually devoid of crystallites suggesting that these crystallites are the product of millerite alteration. (**b**) Enlargement of one of the $NiSO_4$ crystallites on the millerite surface.

anhydrous $NiSO_4$, the difference being largest for the greatest degree of hydration. Even without hydration, the oxidation of NiS to $NiSO_4$ by molecular oxygen has a $\Delta G_{rxn} = -162.6$ kcal/mol. Therefore, the oxidation of NiS to $NiSO_4$ is thermodynamically favored and should occur provided it is kinetically favored.

It should be emphasized that the $NiSO_4$ peaks are relatively broad compared to those of NiS. It is possible that $NiSO_4$, of variable degrees of hydration or containing hydroxyl groups, as well as other oxysulfur species are present at the surface. The presence of these different species with slightly different, unresolved binding energies, would give rise to a broad peak. Because only one peak is used to fit this distribution, the result would be a broad peak.

The second important oxidation product is $Ni(OH)_2$. There were no $Ni(OH)_2$ crystallites observed by SEM/EDX analysis, yet its signal was ubiquitous across the oxidized surface by XPS analysis (Fig. 4 and Fig. 5). The binding energies for the Ni $2p_{3/2}$ and O 1s components are consistent with $Ni(OH)_2$. Once again, as in the case of the $NiSO_4$, the $Ni(OH)_2$ peaks are broader than those of the NiS peaks. This broadening is perhaps due to the presence of more than one hydroxy nickel species, thus giving rise to numerous closely spaced, but unresolved, photopeaks. Auger electron spectroscopy results also confirm the presence of oxygen-enriched surface products as evidenced from the decrease in the oxygen signal following Ar^+ ion bombardment.

The fact that Ni^{2+} and S^{2-} peaks of millerite are observed in the XPS spectra of the 24 h air-reacted sample suggests that the $NiSO_4$ and $Ni(OH)_2$ species form islands with the millerite still exposed around these islands, or that the secondary products form a very thin overlayer (no more than ~1 nm thick). A thin layer would allow photoelectrons from the millerite underlayer to escape and be detected. Island formation is likely for $NiSO_4$ considering the presence of crystallites on the surface of the 1 year air-oxidized sample, but a thin, continuous veneer is more likely for $Ni(OH)_2$ in that it better explains the XPS and SEM observations for the 1 year air-oxidized sample.

A question arises as to why the sulfate forms crystallites whereas the hydroxide forms a coating. Realizing that a thin film of water exists at the surface of the mineral exposed to air, we make some analogies based on aqueous properties of $NiSO_4$ and $Ni(OH)_2$ salts. $NiSO_4$ is highly soluble, whereas $Ni(OH)_2$ has a much lower solubility in near-neutral to basic solutions. Presumably there is sufficient Ni^{2+} and hydroxide available during the early stages of oxidation to allow formation of the $Ni(OH)_2$ everywhere over the surface. Ni^{2+} and sulfate concentrations are too low, however, to produce a uniform layer of $NiSO_4$. Instead, surface diffusion of these species results in local accumulations of Ni^{2+} and sulfate, and ultimately, in the formation of $NiSO_4$ crystallites. The photomicrograph in Figure 6a suggests that minor amounts of Ni^{2+} and sulfate may migrate across the millerite-pentlandite phase boundary to produce very small crystallites on pentlandite close to the phase boundary. There are, however, no crystallites within the central portion of large pentlandite grains.

Coincident with formation of the hydroxy nickel surface complex is the formation of polysulfides. The nickel that reacts with the water and oxygen of ambient air is no longer bonded to sulfide. This sulfide is therefore available to react with other near-surface species, including other sulfide ions, which may lead to the formation of polysulfides (including disulfide) according to the following reaction scheme:

$$n\mathrm{NiS} + (n-1)\mathrm{H_2O} + (n-1)/2\mathrm{O_2} \rightarrow \mathrm{Ni^{2+}\text{-}S_n^{2-}} + (n-1)\mathrm{Ni(OH)_2},$$

where $2 \leq n \leq 8$. The designation Ni^{2+}-S_n^{2-} is used to denote polysulfide bonded to nickel in the lattice at the millerite surface. The $Ni(OH)_2$ and polysulfide may exist as separate, thin layers on the millerite surface with the $Ni(OH)_2$ presumably forming the overlayer. Alternatively, the polysulfides may be intermixed with the $Ni(OH)_2$ in the oxidized overlayer.

The millerite sample exposed to air-saturated de-ionized water for 24 h shows little difference from the vacuum-fractured sample. Because the reactions in air occur with both oxygen and water, and the solution of this experiment is air-saturated, we expect similar products to form. It is likely that $NiSO_4$ and $Ni(OH)_2$ are formed on the surface of the water-reacted sample but do not accumulate; they are instead dissolved by the solution. As support, we expect both $NiSO_4$ and $Ni(OH)_2$ to be relatively soluble at pH values around 6. Polysulfide (5 to 10%) is present on the water-reacted surface, which supports the formation and dissolution of $Ni(OH)_2$, leaving behind a sulfur-rich (relative to nickel) surface.

The formation and subsequent dissolution of reaction products explains the dearth of $NiSO_4$ in the spectra of the water-exposed sample. There is evidence, however, for the presence of a small amount of hydroxy nickel species on the water-reacted surface, although the amount is much less than for the air-reacted samples. The binding energy value for the Ni $2p_{3/2}$ component is consistent with $Ni(OH)_2$, but the O 1s binding energy value (531.9 eV) is 0.4 eV higher than that obtained for the air oxidized samples. This value is also about 0.5 to 1 eV higher than what is expected for bulk $Ni(OH)_2$ based on literature values (Table 2). This surface species has been observed on heazlewoodite, Ni_2S_3, (Buckley and Woods 1991a) as well as nickel-bearing sulfide minerals such as pentlandite (Buckley and Woods 1991b). In both these cases, the interpretation given for this surface species has been that of a hydrated nickel oxide species. This designation seems misleading because it implies that an oxide species is present. No indication exists of an oxide signal in the O 1s spectrum. Binding energy values for the O 1s XPS peak of NiO have been reported in the range of 529.6 and 529.8 eV (Table 2). Mansour and Melendres (1996a) provide XPS spectra for $Ni_2O_3 \cdot 6H_2O$. The O 1s spectrum reveals contributions at binding energy values of 529.3 eV (attributed to Ni_2O_3), 530.8 eV [attributed to $Ni(OH)_2$], and 532.3 eV (attributed to water). The O 1s binding energy for the surface species observed on the water-reacted surface as well as in the study of other nickel-bearing sulfides (Buckley and Woods 1991a, 1991b) is approximately 0.5 to 1 eV higher that expected for a hydroxide species, but is also approximately 0.5 eV lower than expected for adsorbed water species. It is noteworthy that the binding energy of the O 1s peaks increases in the order oxide, hydroxide, chemisorbed water, physisorbed water, and finally water electrically isolated from the surface for most metal oxygen type complexes (Table 2; Knipe et al. 1995). The important aspect is that the stronger the oxygen-metal bond is, the lower the binding energy of the oxygen species will be. It is therefore interpreted that the 531.9 eV peak arises from a hydroxyl group chemisorbed to Ni^{2+} in the lattice at the millerite surface, thus explaining the shift of the O 1s peak to higher binding energy.

The oxidation of pyrrhotite has been well documented (Buckley and Woods 1985; Jones et al. 1992; Pratt et al. 1994a; Pratt et al. 1994b; Mycroft et al. 1995). Under similar conditions to those in our experiments, the main observation derived from the oxidation of pyrrhotite has been the formation of an iron oxyhydroxide (FeOOH) overlayer with a sulfur-rich sub-surface layer (Buckley and Woods 1985; Jones et al. 1992; Pratt et al. 1994a). The mechanism proposed for its oxidation involves diffusion of iron to the surface from the bulk. The presence of a sulfur-rich sub-surface layer has been clearly demonstrated by Auger depth profiling (Pratt et al. 1994a). Although there may be the development of a very thin sulfur-enriched zone beneath the $Ni(OH)_2$ overlayer in our millerite studies, it was not detected by Auger depth profile results. It is consequently uncertain whether the polysulfide occurs as an underlayer to the $Ni(OH)_2$ zone, or whether the polysulfides and hydroxy nickel species are intermixed in the oxidized overlayer. Another important observation is that the $Ni(OH)_2$ is soluble in de-ionized water. This leads to its dissolution during reaction with aqueous solutions in our leaching experiments. Iron oxyhydroxides are not nearly so soluble (Jones et al. 1992). Oxidation of pentlandite in de-ionized water also shows the formation of an insoluble iron oxyhydroxide surface layer (Legrand et al. 1997) and a question arises as to the fate of the hydroxy nickel species.

Conclusions

Millerite Ni $2p_{3/2}$ and S $2p_{3/2}$ binding energies are 853.1 and 161.7 ± 0.2 eV, respectively. Millerite exposed to air and water will react to form various species, the most important of which are hydroxy nickel [$Ni(OH)_2$] and oxysulfur nickel species (mainly hydrated $NiSO_4$). The sulfur in NiS is ultimately oxidized to oxysulfur species (mainly sulfate), although some intermediate polysulfides and perhaps elemental sulfur is produced. The nickel oxidation state remains as Ni^{2+}.

Similar reactions occur in water and air but the $NiSO_4$ and the $Ni(OH)_2$ are soluble and are removed from the surface by dissolution. There remains evidence of polysulfide formation on the water reacted sample. $NiSO_4$ forms on the surface of millerite as discrete crystallites while the $Ni(OH)_2$ probably forms a thin layer covering the entire surface.

Acknowledgments

The authors would like to thank INCO Ltd. for granting D.L. Legrand a leave of absence and financial support to carry out this work. We thank D. Dillon for providing samples, G. Wood for sample preparation, and Y.

Thibault for providing microprobe analysis. We thank the staff at Surface Science Western, especially N.S. McIntyre, R. Davidson, M. Biesinger, and G. Good for use of the facilities and for sharing their expertise. We are indebted to the reviewers of the manuscript and especially to David Vaughan for the many suggestions for improvement and clarification of the text. Financial support through NSERC grants to the last two authors is also acknowledged.

REFERENCES CITED

Bancroft, G.M. and Hyland, M.M. (1990) Spectroscopic studies of adsorption/reduction reactions of aqueous metal complexes on sulfide surfaces. In Mineralogical Society of America Reviews in Mineralogy, 23, 511–558.

Briggs, D. and Rivière, J.C. (1994) Spectral Interpretation. In D. Briggs and M.P. Seah, Eds., Practical Surface Analysis. Volume 1: Auger and X-ray Photoelectron Spectroscopy, (2nd edition), p. 85–141. Wiley, New York.

Broutin, P., Ehrhardt, J.J., Pentenero, A., and Gras, J.M. (1984) Etude micrographique et spectroscopique (Auger et ESCA) de dépots nickel-soufre utilisés comme catalyseurs dans l'électrolyse alkaline de l'eau. Journal de Microscopie et Spectroscopie Electronique, 9, 57–73 (in French).

Buckley, A.N. and Woods, R. (1985) X-ray photoelectron spectroscopy of oxidized pyrrhotite surfaces I. Exposure to air. Applications of Surface Science, 22/23, 280–287.

———(1991a) Electrochemical and XPS studies of the surface oxidation of synthetic heazlewoodite (Ni_2S_3). Journal of Applied Electrochemistry, 21, 575–582.

———(1991b) Surface composition of pentlandite under flotation-related conditions. Surface and Interface Analysis, 17, 675–680.

Buckley, A.N., Wouterlood, H.J., Cartwright, P.S., and Gillard, R.D. (1988) Core electron binding energies of platinum and rhodium polysulfides. Inorganica Chimica Acta, 143, 77–80.

Clifford, R.K., Purdy, K.L., and Miller, J.D. (1975) Characterization of sulfide mineral surfaces in froth flotation systems using electron spectroscopy for chemical analysis. AIChE Symposium Series on Advances in Interfacial Phenomena, 150(71), 138–147.

Cotton, F.A. and Wilkinson, G. (1988) Advanced inorganic chemistry (Fifth edition), 1455 p. Wiley, New York.

Doniach, S. and Sunjic, M. (1970) Many-electron singularity in X-ray photoemission and X-ray line spectra from metals. Journal of Physics C: Solid State Physics, 3, 285–291.

Knipe, S.W., Mycroft, J.R., Pratt, A.R., Nesbitt, H.W., and Bancroft, G.M. (1995) X-ray photoelectron spectroscopic study of water adsorption on iron sulfide minerals. Geochimica et Cosmochimica Acta, 59, 1079–1090.

Jones, C.F., LeCount, S., Smart, R.St.C., and White, T.J. (1992) Compositional and structural alteration of pyrrhotite surfaces in solution: XPS and XRD studies. Applied Surface Science, 55, 65–85.

Laajalehto, K., Kartio, I., Kaurila, T., Laiho, T., and Suoninen, E. (1996) Investigation of copper sulfide surfaces using synchrotron radiation excited photoemission spectroscopy. In H.J. Mathieu, B. Reihl, and D. Briggs, Eds., European Conference on Applications of Surface and Interface Analysis ECASIA'95, p. 717–720. Wiley, Chichester, New York.

Legrand, D.L., Bancroft, G.M., and Nesbitt, H.W. (1997) Surface characterization of pentlandite, $(Fe,Ni)_9S_8$, by X-ray photoelectron spectroscopy. The International Journal of Mineral Processing, 51, 217–228.

Limouzin-Maire, Y. (1981) Etude par spectroscopie ESCA de sulfures et sulfates de manganèse, fer, cobalt, nickel, cuivre et zinc. Bulletin de la société chimique de France, 9–10, I-340–I-342 (in French).

Löchel , B.P. and Strehblow, H.-H. (1984) Breakdown of passivity of nickel by fluoride II. Surface analytical studies. Journal of the Electrochemical Society: Electrochemical Science and Technology, 131, 713–723.

Mansour, A.N. (1996a) Characterization of b-$Ni(OH)_2$ by XPS. Surface Science Spectra, 3, 239–246.

———(1996b) Characterization of NiO by XPS. Surface Science Spectra, 3, 231–238.

Mansour, A.N. and Melendres, C.A. (1996a) Characterization of $Ni_2O_3{\cdot}6H_2O$ by XPS. Surface Science Spectra, 3, 263–270.

———(1996b) Characterization of electrochemically prepared gNiOOH by XPS. Surface Science Spectra, 3, 271–278.

Matienzo, L.J., Yin, L.O., Grim, S.O., and Swartz, W.E. Jr. (1973) X-ray photoelectron spectroscopy of nickel compounds. Inorganic Chemistry, 12, 2762–2769.

McIntyre, N.S. and Cook, M.G. (1975) X-ray photoelectron studies on some oxides and hydroxides of cobalt, nickel, and copper. Analytical Chemistry, 47, 2208–2213.

Mycroft, J.R., Bancroft, G.M., McIntyre, N.S., Lorimer, J.W., and Hill, I.R. (1990) Detection of sulfur and polysulfides on electrochemically oxidized pyrite surfaces by X-ray photoelectron spectroscopy and Raman spectroscopy. Journal of Electroanalytical Chemistry, 292, 139–152.

Mycroft, J.R., Nesbitt, H.W., and Pratt, A.R. (1995) X-ray photoelectron and Auger electron spectroscopy of air-oxidized pyrrhotite: Distribution of oxidized species with depth. Geochimica et Cosmochimica Acta, 59, 721–733.

Pratt, A.R., Muir, I.J., and Nesbitt, H.W. (1994a) X-ray photoelectron and Auger electron spectroscopic studies of pyrrhotite and mechanism of air oxidation. Geochimica et Cosmochimica Acta, 58, 827–841.

Pratt, A.R., Nesbitt, H.W. and Muir, I.J. (1994b) Generation of acids from mine waste: Oxidative leaching of pyrrhotite in dilute H_2SO_4 solutions at pH 3.0. Geochimica et Cosmochimica Acta, 58, 5147–5159.

Richardson, S. and Vaughan, D.J. (1989) Surface alteration of pentlandite and spectroscopic evidence for secondary violarite formation. Mineralogical Magazine, 53, 213–222.

Salvati, L. Jr., Makovsky, L.E., Stencel, J.M. Brown, F.R., and Hercules, D.M. (1981) Surface spectroscopic study of tungsten-alumina catalysts using X-ray photoelectron, ion scattering, and Raman spectroscopies. Journal of Physical Chemistry, 85, 3700–3707.

Scofield, J.H. (1976) Hartree-Slater subshell photoionization cross-sections at 1254 and 1487 eV. Journal of Electron Spectroscopy and Related Phenomenon, 8, 129–137.

Shalvoy, R.B. and Reucroft, P.J. (1979) Characterization of a sulfur-resistant methanation catalyst by XPS. Journal of Vacuum Science and Technology, 16, 567–569.

Shirley, D.A. (1972) High-resolution X-ray photoemission spectrum of the valence bands of gold. Physical Review B, 5, 4709–4714.

Termes, S.C., Buckley, A.N., and Gillard, R.D. (1987) 2p electron binding energies for the sulfur atoms in metal polysulfides. Inorganica Chimica Acta, 126, 79–82.

Vaughan, D.J. and Craig, J.R. (1978) Mineral Chemistry of Metal Sulfides, 493 p. Cambridge University Press. Cambridge, U.K.

MANUSCRIPT RECEIVED NOVEMBER 19, 1997
MANUSCRIPT ACCEPTED JUNE 23, 1998
PAPER HANDLED BY GLENN A. WAYCHUNAS